SAND2000-2290C

Constitutive Model Development for Predicting Thermal Mechanical Fatigue Deformation in Solder Interconnects‡

P. Vianco
A. Fossum
M. Neilsen
S. Burchett
Sandia National Laboratories
Albuquerque, NM

Abstract
A unified creep-plasticity (UCP) model was developed to describe the deformation of 97In-3Ag (wt.%) solder for the purpose of predicting thermal mechanical fatigue in electronic interconnects. The UCP model uses a hyperbolic sine function of effective stress in its kinetic equation for the inelastic strain rate. Compression stress-strain and compression creep experiments were performed on bulk, as-fabricated 97In-3Ag solder samples to obtain the necessary materials properties. Yield stress and elastic modulus parameters were calculated. Compression creep experiments were performed at the same temperatures to provide the sinh law exponent and apparent activation energy of deformation. The measured properties and parametric optimization yielded a constitutive equation having a very good fit to both the slow and fast strain rate, compression stress-strain curves at all test temperatures.

Introduction

The shift in electronics assembly from through-hole technology to surface mount technology brought about an increased realization of the susceptibility of 63Sn-37Pb (wt.%) or 60Sn-40Pb solders to fatigue damage. The reduced size of the surface mount solder joint increases the stresses and strains placed on the solder fillet under *mechanical fatigue* conditions. More critical, however, is fatigue damage introduced into the solder by thermal cycling environments. Temperature fluctuations cause stresses and strains in the solder as a consequence of the thermal expansion mismatches between the electronic package, package I/O, the solder, and the substrate that comprise the overall joint structure. Because mechanical loads *and* temperature both impact the fatigue response of the solder, this degradation mode is termed *thermal mechanical fatigue (TMF)*.

When the susceptibility to TMF by surface mount solder joints became evident, the electronics community performed extensive accelerated aging studies to document the TMF behavior of Sn-Pb solder. Large facilities of temperature cycling furnaces were established; each furnace holding "reliability" test vehicles containing arrays of leadless and leaded surface mount packages that were electrically connected in "daisy chain" patterns. The electrical signals were fed to banks of data loggers that recorded "opens" indicating that a cracked solder joint had formed. The rate at which solder joint opens occurred established the statistical framework from which the reliability of each package configuration was predicted. In addition, failure mode analysis (FMA) performed on the open solder joint identified the microstructural features that characterized TMF deformation and crack propagation in the Sn-Pb solder. For example, laboratory studies confirmed many of the qualitative and quantitative aspects of TMF in Sn-Pb solder, including the localized band of Pb-rich phase coarsening that became the signature morphology of TMF in this solder[1].

The resources that were used to establish this extensive, empirical database describing the TMF of Sn-Pb solder joints will not be available for quantifying the reliability of Pb-free solders. The vast number of available packages and I/O

‡ Sandia is a multiprogram laboratory operated by Sandia Corporation, a Lockheed Martin Company, for the US Dept. of Energy under Contract AC04-94AL85000. This work was supported in large part by a Work for Others Project with the US. Army, AMCOM, Redstone Arsenal, AL.

DISCLAIMER

DISCLAIMER

Portions of this document may be illegible in electronic image products. Images are produced from the best available original document.

configurations, as well as the increasing number of new package designs, will make such an effort daunting. Also, the present business environment within the electronics industry poses two additional constraints. First, reduced budgetary resources create a significant roadblock against extensive experimental programs. Secondly, the shift in circuit board technology from the OEMs, who traditionally did interconnect research and development, to contract manufacturers, has left a gap in terms of which party is responsible for performing those empirical programs that would be required to establish the reliability databases for Pb-free solder compositions. As a consequence, there will need to be a greater emphasis placed on the use of computational models to develop reliability data for Pb-free soldered interconnects.

The computational approach used to develop a reliability prediction tool is comprised of the following three tasks: (1) determine the pertinent materials properties of the solder (elastic modulus, yield strength, etc.) over the applicable temperature range; (2) construct the solder alloy constitutive model (equation) from the materials properties and combine it with the solder joint (I/O) finite element mesh to complete the overall TMF computational model; and (3) perform a limited number of accelerated aging (thermal cycling) experiments on prototype interconnects to validate the model predictions. This report will describe the studies that were performed to determine the materials properties [step (1)] and then to develop the constitutive model [first part of step (2)] for the low melting temperature solder 97In-3Ag wt.%).

The particular constitutive model used in this study was based upon a unified creep-plasticity (UCP) approach. That is, there is no separation of creep and plastic strains and instead, they are combined and referred to as simply inelastic strain. A one-dimensional form of the kinetic equation which describes the relationship between the inelastic strain rate and stress is shown as equation (1)[2].

$$d\varepsilon_{11}/dt = \mathrm{sgn}(\sigma_{11}-B_{11}) f_o \exp(-Q/RT) \sinh^p[(/\sigma_{11}-B_{11}/)/\beta D] \quad (1)$$

where: $d\varepsilon_{11}/dt$ is the inelastic strain rate (s^{-1}) and σ_{11} is the applied stress (MPa). The strain variables and B_{11} and D represent the back stress and isotropic strength, respectively. Evolution of the state variables is defined by several material parameters (A_i) through the following expressions:

$$dD/dt = (A_1|d\varepsilon^p_{11}/dt|)/(D-D_o)^{A3} - A_2(D-D_o)^2 \quad (1a)$$

$$dB_{11}/dt = (A_4|d\varepsilon^p_{11}/dt|)/|B_{11}|^{A6} - A_5 B_{11}|B_{11}| \quad (1b)$$

Referring to equation (1), the parameters determined from the creep tests include: f_o (1/MPa-s); Q, the apparent activation energy (J/mol); and p, the sinh term exponent. Other parameters include: β, a numerical constant; T, the temperature (°K); and R, the universal gas constant (8.314 J/mol-°K). The subscript "11" denotes the uniaxial (1-D) case in which the applied stress and deformation occur in the same (x) direction. The one-dimensional equations shown above are generalized to the three-dimensional case in the normal way by assuming that the inelastic deformation is purely deviatoric. A complete description of the three-dimensional constitutive model can be found in Reference 2.

The solder, 97In-3Ag, is a eutectic composition of the In - Ag binary alloy system; the melting temperature is 143°C. The relatively high cost of In and Ag limits the use of In-Ag solder to niche applications such as high-reliability, space or military hardware which is often characterized by very limited production numbers. The use of In-Ag solder for space applications is also attributed to its very high ductility at cryogenic temperatures. Because of limited applications, there has not been an impetus to develop an extensive properties database for this material. Time-independent mechanical properties were not located. Time-dependent deformation studies in the form of constant load *shear* creep tests were performed on 97In-3Ag solder *joints* by Reynolds, et al. over the temperature range of 0°C to 90°C and applied shear stresses of 0.4 to 25 MPa[3].

In order to develop both time-independent (stress-strain) and time-dependent (creep) material properties with which to build a computational model of the 97In-3Ag solder, the compression test methodology was used. The stress-strain test data were analyzed for the elastic modulus (E) and yield stress(σ_y) parameters as a function of temperature and displacement (strain) rates. Later in the analysis, the stress-strain data were used in a fitting routine with the constitutive equation (1) in order to adjust the remaining parameters. The yield strength data were also used to establish the nominal (initial) stresses for the constant load creep tests to determine f_o, Q, and p for equation (1).

Experimental procedures - sample fabrication

The sample geometry that was selected for both stress-strain and creep tests was that of a cylinder. The specimens were fabricated by the following

procedure (Fig. 1). First, a suitable quantity of 97In-3Ag solder (having a certified composition) was melted into a small pot. The molten solder was then poured into a bullet mold and allowed to solidify.

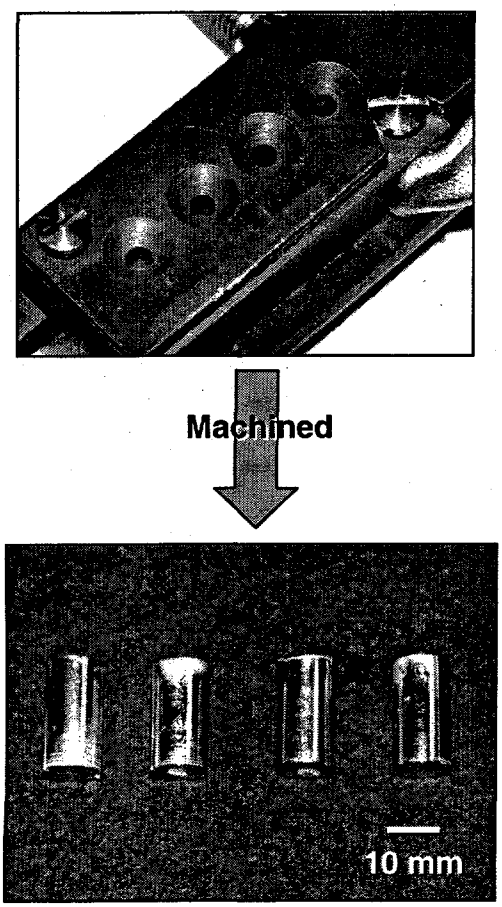

Figure 1. Fabrication process used to make the test samples.

Each of the four holes in the mold had been modified to give the as-cast samples slightly larger than nominal dimensions. The samples were extracted from the mold and then weighed on a precision balance in order to screen out those cylinders with excessive void formation. Each sample was machined to the nominal finished dimensions of 10 mm in diameter and 19 mm in length. The exact dimensions of each sample were measured and catalogued for subsequent data analyses. Although the ASTM standard recommends the so-called "medium length" ratio of 3.0 for general properties measurements, the diameter and length were chosen to adhere to the "short length" ratio of 2.0 due to the softness of the material[4].

The data presented in this report pertain to samples tested in the *as-fabricated* condition. Tests were also performed on cylinders that were aged at 67°C for 8, 16, or 24 hours; those data and follow-up analyses will be presented in a future publication.

Experimental procedures – time independent (stress-strain) tests and data analysis

The stress-strain compression tests were performed on a servo-hydraulic frame. All tests were performed in duplicate. The test temperatures were –25°C, 25°C, 75°C, and 125°C. The temperature of the test sample was controlled to $\pm$0.5C° by passing suitably heated or cooled gas through the platens that contacted the top and bottom surfaces of the sample cylinder. A negligible temperature gradient along the cylinder length was verified by thermocouple measurements. A photograph of the experimental set-up is shown in Fig. 2. The tests were performed at one of two displacement rates: 0.05 mm/min or 1.0 mm/min. These cross-head speeds correspond to strain rates of 4.2×10^{-5} s^{-1} and 8.3×10^{-4} s^{-1}, respectively, as experienced by the samples. The engineering yield stress from each test was determined by the 0.2% offset criterion[4]. The elastic modulus was calculated from the constant slope portion of the load-displacement curve, using the initial area and length of the specimen as per the ASTM test procedure E111[5].

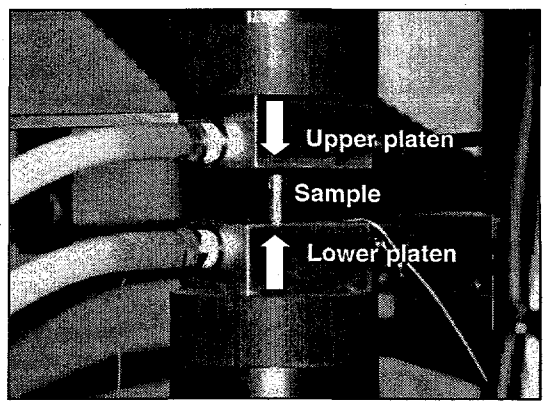

Figure 2. Experimental set-up used for both the stress-strain and creep testing.

Experimental procedures – time dependent (creep) tests and data analysis

The test procedure was developed from ASTM E139-96 [6]. The same test frame configuration as shown in Fig. 2 was used for the creep tests. However, in the latter case, a constant load was applied to the sample and the sample deformation recorded as a function of time. That load was based upon the yield stress of the In-Ag solder measured at the same temperature as were used in the stress-strain tests: –25°C, 25°C,

75°C, or 125°C. Nominal stresses were computed from 20%, 40%, 60%, and 80% of the respective yield stress value. The creep experiments were performed in duplicate per each test condition.

Sample data analysis was performed in the following manner. First, the (digital) displacement-time plots were converted into strain-time graphs. Then, a three point difference method was used to convert the strain-time graphs into strain rate-time plots. The minimum strain rate was then calculated from the latter plots. In addition, the true stress responsible for the minimum strain rate was computed, based upon the initial stress and a constant volume change to the cross sectional area resulting from creep deformation. Next, the data were fit to a simplified version of constitutive equation (1) that excluded variations in the material state. Equation (2) was used to obtain the initial estimate of the time dependent parameters (f_o, p, and Q):

$$d\varepsilon/dt = f_o \sinh^p[(\alpha\sigma]\exp(-Q/RT) \qquad (2)$$

The parameters in equation (2) were obtained by a multivariable least-squares analysis routine that was performed on the logarithm of equation (2). The independent variables were $\ln\{\sinh[(\alpha\sigma]\}$ and $1/T$; the dependent variable was $\ln(d\varepsilon/dt)$. The fit routine was performed with different values of α the optimum value was that which maximized R^2 for the fit.

The construction of the UCP constitutive equation (1) began by introducing the time independent and time dependent parameters into the function. Then, equation (1) was fit to the stress-strain curves representing both slow and fast strain rate conditions. A comparison of the computational stress-strain curves from equation (1) with their empirical counterparts was used to adjust the fitting parameters in order to realize a best agreement between the computational and experimental cases.

Results and discussion - stress-strain tests

Shown in Fig. 3 are representative stress-strain curves for the as-fabricated 97In-3Ag solder sample tested at –25°C, 25°C and 125°C under the strain rate of 4.2×10^{-5} s^{-1}.

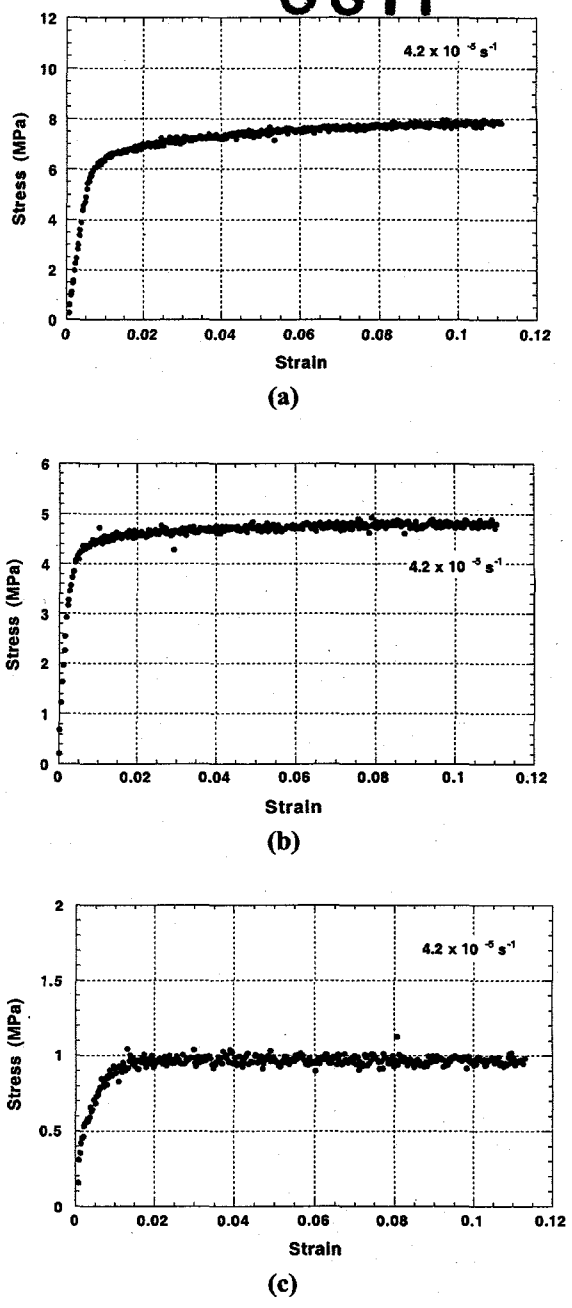

Figure 3. Stress-strain curves of In-Ag samples recorded for tests performed at a strain rate of 4.2 x 10^{-5} s^{-1} and temperatures of: (a) –25°C, (b) 25°C, and (c) 125°C.

Aside from the expected decrease in strength with increased temperature, there were no other unusual load response behaviors by the material. The stress-strain curve for the 25°C test performed under a strain rate of 8.3×10^{-4} s^{-1} is shown in Fig. 4. Again, the plots resulting from tests performed at –25°C as well as 75°C and 125°C did not indicate any

distinguishable behaviors resulting from the higher strain rate.

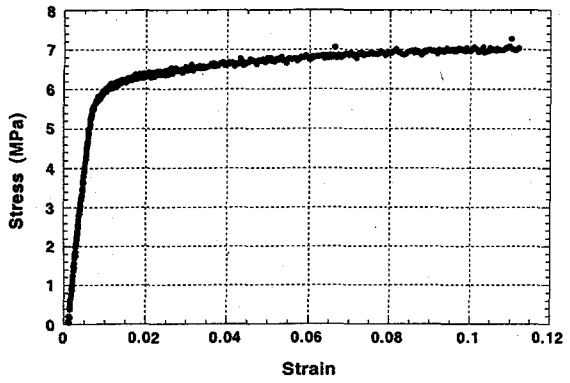

Figure 4. Stress-strain curve of an In-Ag sample recorded at 25°C and a strain rate of 8.3 x 10^{-4} s^{-1}.

The yield stress and elastic modulus properties were obtained as a function of strain rate and temperature. The yield stress data are shown in Figs. 5a and 5b, each plot representing one of the two strain rate conditions. Shown as gray circles in each plot are the two values obtained from the duplicating experiments; the black circle is the mean of those two values. The absolute error of each individual data point (i.e., the gray circles) is commensurate with the size of the symbols.

As expected, the yield stress values exhibited a monotonic decrease with test temperature for both strain rate conditions. The trend at the lower strain rate exhibited a quadratic dependence between yield stress and temperature while at the higher strain rate, a linear dependence was most suitable. The yield stress values were lower at the reduced strain rate; however, that difference gradually diminished with increased test temperature.

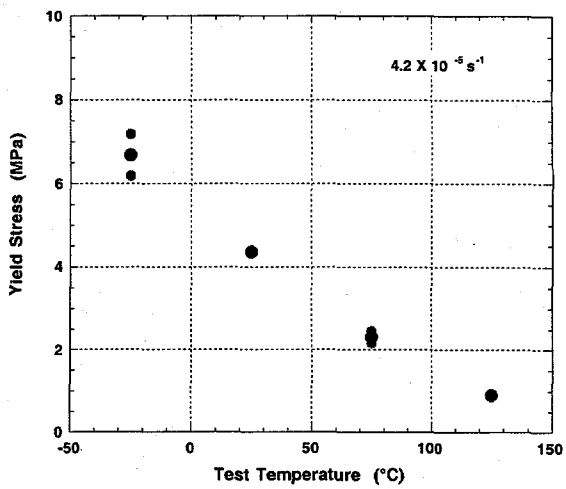

(a)

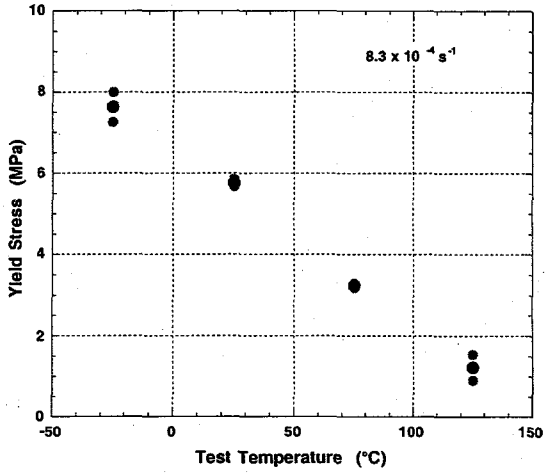

(b)

Figure 5. Yield stress (MPa) of the as-fabricated 97In-3Ag solder samples as a function of test temperature for the two strain rates: (a) 4.2 x 10^{-5} s^{-1} and (b) 8.3 x 10^{-4} s^{-1}.

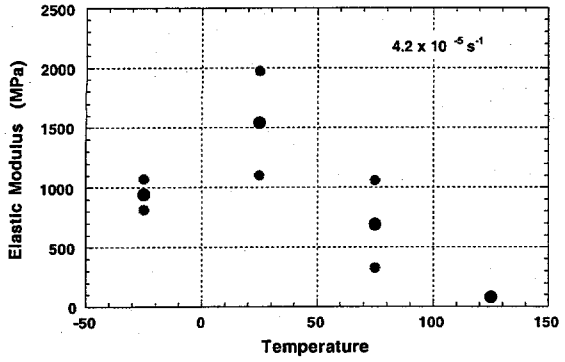

(a)

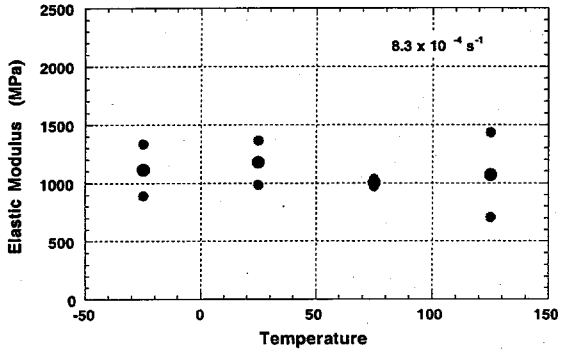

(b)

Figure 6. Elastic modulus (MPa) of the as-fabricated 97In-3Ag solder samples as a function of test temperature for the two strain rates: (a) 4.2 x 10^{-5} s^{-1} and (b) 8.3 x 10^{-4} s^{-1}.

The elastic modulus data are provided in Fig. 6. It was expected that the elastic modulus would monotonically decrease with increased temperature. However, at the lower strain rate of 4.2 x 10^{-5} s^{-1} (Fig. 6a), the elastic modulus increased from the –25°C to the 25°C test condition; it then monotonically decreased for the higher temperatures. There was no peculiarity in the respective stress-strain curves (see Figs. 3a and 3b) that would suggest such a behavior. It can only be hypothesized that an allotropic change (e.g., an order-disorder reaction) may have occurred at a temperature between –25°C and 25°C. Unfortunately, there is insufficient phase diagram information or archived data to support this hypothesis. At the higher strain rate of 8.3 x 10^{-4} s^{-1}, a similar trend was implied by the data (Fig. 6b), but with a considerably reduced magnitude as compared to the slower strain rate results. At the higher strain rate, the modulus did not significantly decrease with test temperature as was anticipated.

Finally, a comparison was made of the elastic moduli between the different strain rate regimes. Given the experimental error inherent in measuring this property, the values of E can be considered similar for the test temperatures of –25°C, 25°C, and 75°C. However, the modulus value measured at 125°C and a strain rate of 4.2 x 10^{-5} s^{-1} was considerably less than that computed for the 125°C temperature, 8.3 x 10^{-4} s^{-1} strain rate experiments. The cause of the discrepancy in this case would most likely rest with the difficulty of identifying the elastic portion of the high temperature, stress-strain curves. Therefore, it would be expected that the elastic modulus of the 97In-3Ag solder at 125°C would lie between the mean values computed at the two strain rates.

Results and discussion - creep tests

Shown in Fig. 7 are representative displacement-time curves for creep tests performed with the 97In-3Ag solder. The particular plots shown in the figure were obtained under the following test conditions of temperature and initial or nominal stress: (a) –25°C, 4.61 MPa; (b) 25°C, 2.25 MPa; and (c) 125°C, 0.491 MPa. The creep deformation at –25°C was primarily in the primary regime in which the strain rate decreases with time. This point is illustrated in Fig. 8a which shows both the strain rate and stress as a function of time. The time dependent change in stress occurs as a result of deformation to the sample that causes a change to the cross sectional area of the cylinder. A mean strain rate and mean stress values were calculated from the respective data contained within the range established by the vertical markers; those mean values served as the minimum creep rate, $d\varepsilon/dt_{min}$, and the applied stress, σ, for that particular sample/creep test. The numbers in parentheses represent one standard deviation of the data compiled between the markers. Creep tests performed at 25°C (Fig. 8b), 75°C (not illustrated) and 125°C (Fig. 8c) were comprised largely of secondary or steady state deformation which is characterized by the minimum strain rate condition. The same analyses to obtain $d\varepsilon/dt_{min}$ and σ were applied to these plots, as well.

The strain rate, stress, and temperature parameters were fit to equation (2) as described earlier, selecting the value of α that maximized the R^2 parameter. The optimum value of α was 1.075 MPa^{-1}. The form of equation (2) for the minimum or steady state strain rate as a function of stress and temperature was:

$$(d\varepsilon/dt)_{min} = 2.824 \times 10^{8} \sinh^{3.2}[(1.075\sigma] \exp(-98762/RT) \quad (3)$$

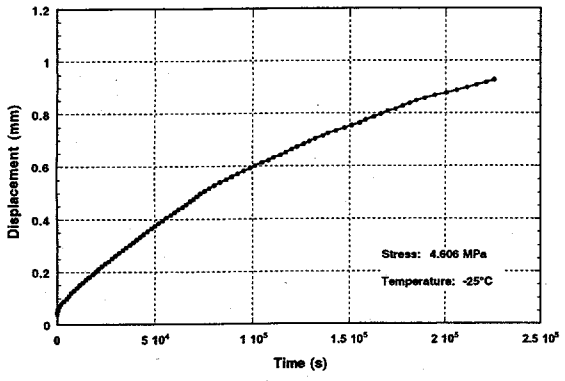

(a)

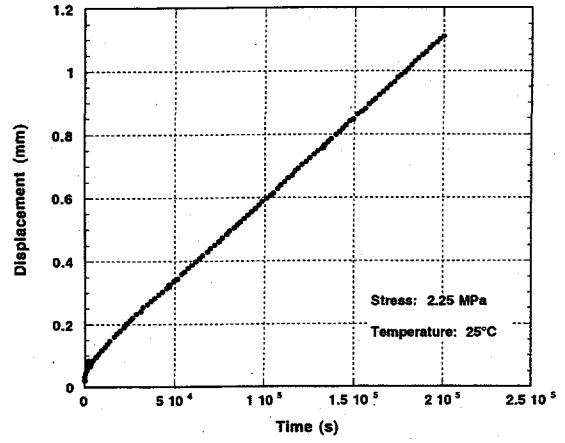

(b)

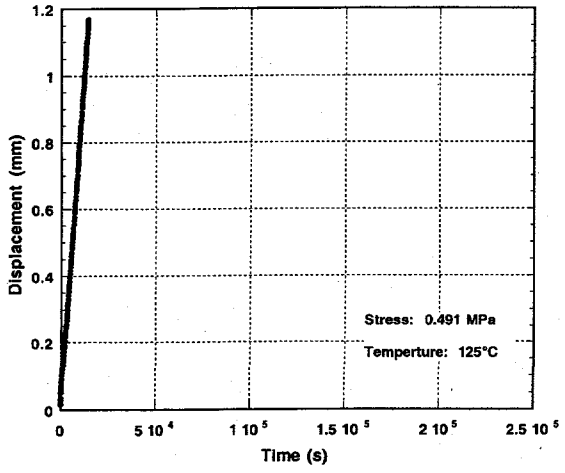

(c)

Figure 7. Creep curves for the as-fabricated 97In-3Ag samples tested at the following temperatures and initial or nominal stress values: (a) –25°C, 4.61 MPa; (b) 25°C, 2.25 MPa; and (c) 125°C, 0.491 MPa.

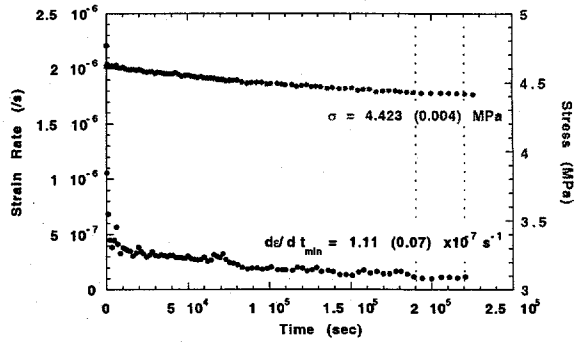

(a)

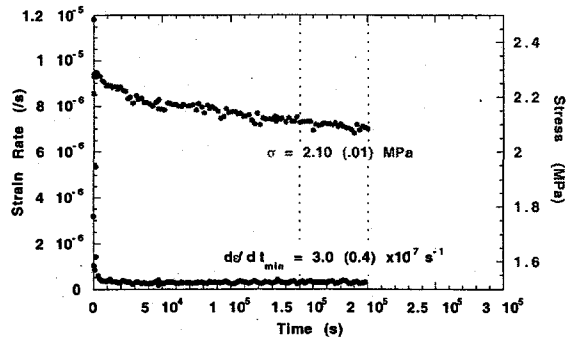

(b)

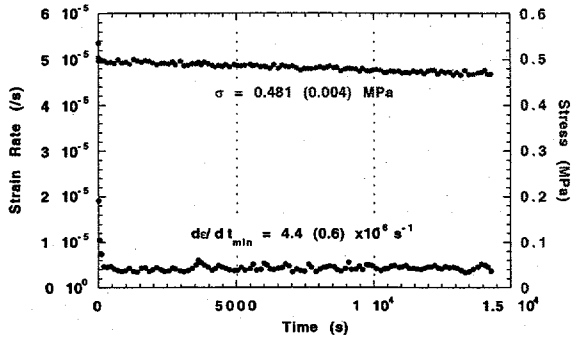

(c)

Figure 8. Strain rate and stress as a function of time for the as-fabricated 97In-3Ag samples tested at the following temperatures and initial or nominal stress values: (a) –25°C, 4.61 MPa; (b) 25°C, 2.25 MPa; and (c) 125°C, 0.491 MPa.

The mean and (±)95% confidence interval values of the sinh term exponent p and the apparent activation energy Q were: 3.2±0.6 and 99±15 kJ/mol, respectively.

The value of p falls between the 2.5 and 6.2 values measured by Reynolds, Kang, and Morris that represented the "low stress" and "high stress" regimes of shear creep in the 97In-3Ag solder[3]. Such

a partitioning of the current compression creep data was not performed for this report. The value of Q was higher than the 81 kJ/mol observed by the aforementioned authors for their "high stress" test regime which was closest to the test conditions used in the present study. Therefore, although the compression creep experiments on bulk 97In-3Ag solder exhibited kinetics parameters that were comparable to those observed in creep shear tests in *Reference [3], some nominal differences remained* between the two data sets that may be attributed to the different testing modes.

Results and discussion - UCP constitutive model (equation)

The stress-strain and compression creep data were used to establish the UCP constitutive equation for 97In-3Ag solder. First, a fit was performed with only the slower strain rate (4.2×10^{-5} s^{-1}) data. The parameters calculated for equations (1), (1a) and (1b) from stress-strain and creep testing are listed here (SI units): $f_o = 2.824 \times 10^8$; $p = 3.2$; $\beta = 1.0$; $D_o = 0.82488$; $A_1 = 2.1542$; $A_2 = 2.5615 \times 10^{-3}$; $A_3 = 1.4442$; $A_4 = A_5 = A_6 = 0.0$; and $Q = 9.8766 \times 10^4$. An excellent fit between the model prediction and the actual test data is demonstrated in Fig. 9.

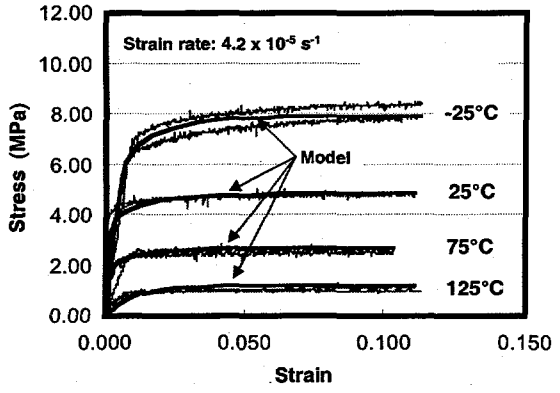

Figure 9. Constitutive model (equation) prediction and actual stress-strain test data for the 97In-3Ag solder (as-fabricated) at the 4.2×10^{-5} s^{-1} strain rate and noted test temperatures.

When the same model prediction was applied to the stress-strain data taken at 8.2×10^{-4} s^{-1}, the goodness of fit had diminished, more so as the test temperature increased. Nevertheless, the correlation between the model and the empirical data was considered to be quite good given the nearly two orders of magnitude difference in the strain rates. The fitting parameters in the constitutive equation were modified in order to improve the fit to both the 4.2×10^{-5} s^{-1} and 8.3×10^{-4} s^{-1} data sets. The resulting parameters for equations (1), (1a), and (1b) were (SI units): $f_o = 2.824 \times 10^8$; $p = 3.2$; $\beta = 1.0$; $D_o = 0.8517$; $A_1 = 0.7146$; $A_2 = 2.269 \times 10^{-3}$; $A_3 = 2.1138$; $A_4 = A_5 = A_6 = 0.0$; and $Q = 9.8766 \times 10^4$.

As a final technique to improve the fit between experiment and the model, the value of β was allowed to be a function of temperature. This approach did vastly improve the fit, particularly at those higher temperatures. The discrete values for β that provided an optimum fit per each test temperature were: 1.0, -25°C; 1.0; 25°C; 0.91303, 75°C,; and 0.71656, 125°C; the other parameters were not changed. The model predictions along with the experimental stress-strain data per each of the two strain rates and four test temperatures are provided in Fig. 10. The corroboration between the constitutive model and the experimental data was very good, although there is a slight loss in the goodness-of-fit as the test temperature was increased. Therefore, a UCP constitutive model was developed to represent time independent and time dependent deformation in the as-fabricated 97In-3Ag solder material. This equation can then be coupled into the finite element mesh of a particular solder joint configuration in order to predict the distribution of TMF deformation in the solder leading up to crack initiation and subsequent propagation that causes interconnect failure.

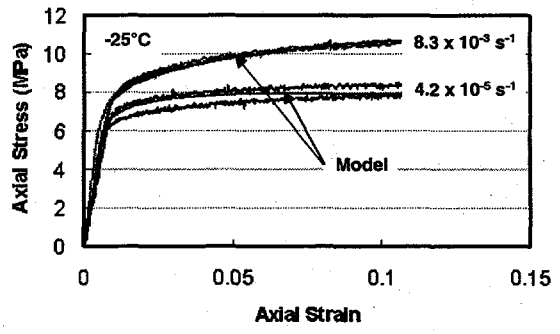

(a)

Figure 10. The 97In-3Ag solder (as-fabricated) stress-stain test data taken at both 4.2×10^{-5} s^{-1} 8.3 x 10^{-4} s^{-1} strain rates and the corresponding unified creep plasticity model predictions for the test temperatures of: (a) –25°C, (b) 25°C, (c) 75°C, and (d) 125°C. ***(con't)***

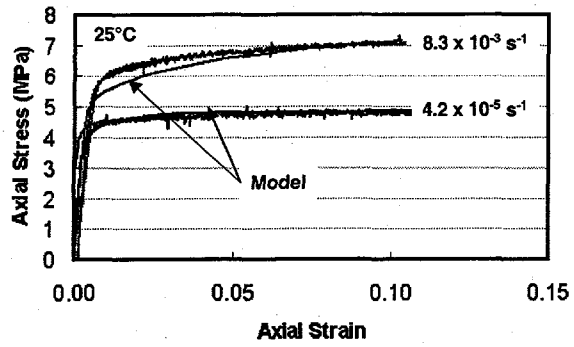

(b)

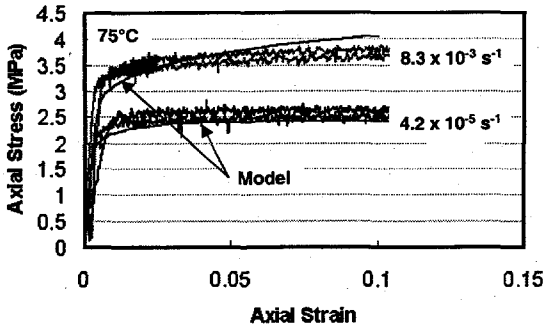

(c)

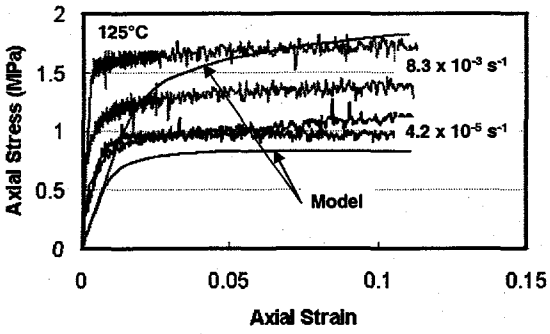

(d)

Figure 10. The 97In-3Ag solder (as-fabricated) stress-stain test data taken at both 4.2 x 10^{-5} s^{-1} 8.3 x 10^{-4} s^{-1} strain rates and the corresponding unified creep plasticity model predictions for the test temperatures of: (a) –25°C, (b) 25°C, (c) 75°C, and (d) 125°C.

The next step in the UCP model development would be to address its "calibration." Prototype interconnects would be fabricated with the In-Ag solder, either via a laboratory test specimen or through the use of actual circuit board assemblies. The test vehicle would then be thermally cycled. The solder joints would be analyzed to identify the number of cycles leading up to crack initiation, thereby establishing the maximum extent of TMF deformation in the solder. This maximum TMF deformation would represent the "failure criterion" to which the model is calibrated after it had been exercised for the same thermal cycling environment and interconnect geometry.

Finally, once the TMF deformation failure criterion has been established, the model must then be validated. That is, a number of laboratory samples or circuit board prototypes would be subjected to a matrix of thermal cycling conditions. The constitutive model of those solder joints would next be exercised for the same matrix of thermal cycling conditions. The number of cycles leading to the onset of cracking in the test vehicle solder joints, which signifies that the criterion of maximum TMF deformation has been reached, would be compared to the predictions established by the model. This comparison would establish the accuracy with which the coupled UCP model and finite element technique can predict TMF deformation is any 97In-3Ag solder interconnect geometry and any temperature environment.

Conclusions

1. A unified creep-plasticity (UCP) model was sought to describe the deformation of 97In-3Ag (wt.%) solder for the purpose of predicting thermal mechanical fatigue (TMF) in electronic interconnects. This model used a hyperbolic sine function of effective stress in its kinetic equation for the inelastic strain rate.

2. Compression stress-strain and compression creep experiments were performed on bulk, as-fabricated 97In-3Ag solder samples to obtain the material parameters for the new model. The stress strain experiments were performed at 4.2 x 10^{-5} s^{-1} and 8.3 x 10^{-4} s^{-1} strain rates and temperatures of –25°C, 25°C, 75°C, and 125°C. Yield stress and elastic modulus parameters were calculated for the constitutive equation.

3. Compression creep experiments were performed at the same temperatures and nominal stresses reflecting 20%, 40%, 60%, and 80% of the yield stress. Those experiments provided the sinh law exponent and apparent activation energy of deformation.

4. The measured properties, along with optimization of the remaining fitting parameters, were used to develop a UCP constitutive equation that accurately describes both the slow and fast strain rate, compression stress-strain curves at each test temperature.

References

[1] D. Frear, "Thermomechanical Fatigue in Solder Materials," *Solder Mechanics - A State of the Art Assessment* ed. by D. Frear, W. Jones and K. Kinsman (TMS, Warrendale, PA; 1991), pp. 191 - 237.

[2] M. Neilsen, S. Burchett, C. Stone, and J. Stephens, "A Viscoplastic Theory for Braze Alloys," *Sandia Report* SAND96-0984 (Sandia National Laboratories, Albuquerque, NM; 1996).

[3] H. Reynolds, S. Kang, and J. Morris, "The Creep Behavior of In-Ag Eutectic Solder Joints," *Journal of Electronic Materials* 28 (1999), pp. 69-75.

[4] "Standard Test Methods for Compression Testing of Metallic Materials at Room Temperature," *ASTM E9-89A* (American Society for Testing and Materials, West Conshohoken, PA; 1995), pp. 101-103.

[5] "Standard Test Methods for Young's Modulus, Tangent Modulus, and Chord Modulus," *ASTM E111-82* (American Society for Testing and Materials, West Conshohoken, PA; 1995).

[6] "Standard Test Methods for Conducting Creep, Creep-Rupture, and Stress-Rupture Tests of Metallic Materials," *ASTM E139-96* (American Society for Testing and Materials, West Conshohoken, PA; 1995).